Caltech
California Institute of Technology
Pasadena, CA 91125

ligo memorandum

TO: Distribution

DATE: 9 August, 1990

FROM: Robert Spero

MAIL STOP/TELEPHONE: 130-33/4437

FILE: to-all

SUBJECT: COINCIDENCE SENSITIVITY

The attached latest (and probably last) draft of my coincidence sensitivity calculation is relevant to the August 30 Review agenda item "Multi-site Coincidence Sensitivity." Hint to the reader pressed for time: Section 5, *Sensitivity as a Function of Orientation*, has the most important results.

RES

Enclosure: "Sensitivity of Two-Way Coincidence Measurements, as Related to Site Selection," 6'th Draft

Distribution:
A. Abramovici
M. Burka
R. Drever
S. Kawamura
F. Raab
D. Shoemaker
M. Zucker

Sensitivity of Two-Way Coincidence Measurements, as Related to Site Selection

R. Spero

1 August, 1990
6'th Draft

Abstract

The burst sensitivity of spatially separated interferometers operated in coincidence is investigated. The sensitivity to linearly polarized waves is presented as a function of separation, orientation, and fractional sky coverage. Specific candidate site pairs are considered.

1. The Method

The method and some of the analysis is after work done by Stan Whitcomb in 1985. The calculation is based on filling a spherical shell on the sky with unit sources distributed evenly in $\cos\theta$, ϕ, and wave polarization Ω. For the results presented here, on the order of 10^6 sources are used for each set of geometrical parameters.

Figures 1 and 2 show the relevant angles: μ_1 and μ_2 specify the orientation for two spatially separated interferometers, $2a$ is the angle between the interferometer planes, and s_1 and s_2 are the angles between one interferometer arm and the line of intersection of the planes. The great-circle arc[1] between the sites is ψ.

Designating by $\hat{a}$ and $\hat{b}$ the unit vectors pointing in the directions of the two arms and by $\hat{x}_w$ and $\hat{y}_w$ the unit vectors along the stretch and shrink axes of a wave traveling in the $\hat{z}_w$ direction, the response of one interferometer (in the low-frequency limit, where the arm lengths are shorter than a gravitational wavelength) is proportional to[2]

$$F_+ = \left[(\hat{a}\cdot\hat{x}_w)^2 - (\hat{a}\cdot\hat{y}_w)^2\right] - \left[(\hat{b}\cdot\hat{x}_w)^2 - (\hat{b}\cdot\hat{y}_w)^2\right] \tag{1}$$

The computer code used translates latitude, longitude, and μ_1 and μ_2 into the natural angular coordinates of Figure 2. A Euler transformation is made between the interferometer frame and the wave frame to calculate the detected strength of each unit source. Figures 3

[1]The great-circle distance is $R_\oplus\psi$, where $R_\oplus$=6400 km.

[2]Equation 1 follows from, for example, applying Equation 2.13 of Reference [1] to two interferometer arms separately, and subtracting.

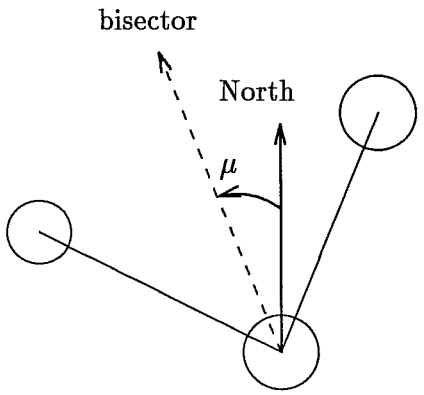

Figure 1: The "bisector angle" μ is measured relative to the local compass North. It is positive toward the East.

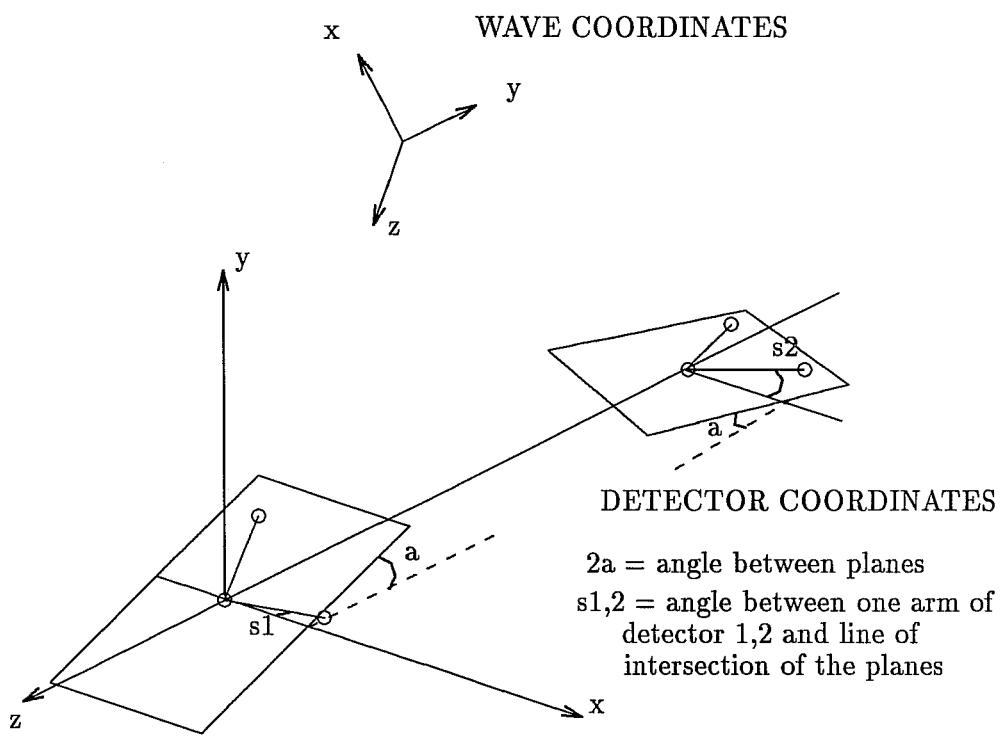

Figure 2: Coordinate system for two interferometers.

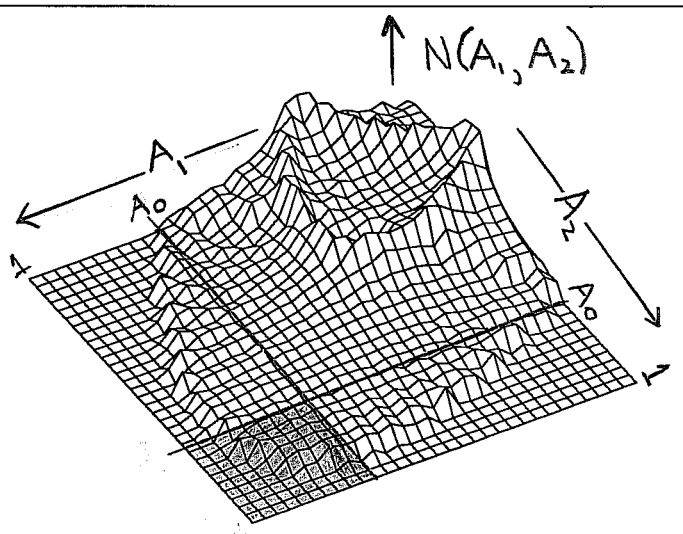

Figure 3: Two-dimensional histogram for spatially coincident interferometers, with relative rotation of 22.5°. The height above the plane $N(A_1, A_2)$ represents the number of events detected with strength (absolute value of amplitude) A_1 in the first interferometer of the pair, and strength A_2 in the second. The shaded region represents those signals above the threshold A_0 in both interferometers. The total number of events in the shaded region divided by all the events (corresponding to $A_0 = 0$) is the "fractional sky coverage" x.

and 4 show sample raw results of these calculations in the form of two-axis histograms. A_1 and A_2 in these figures are the values of F_+ in the first and second interferometer, respectively.

Figure 3 is for two interferometers at the same site, with their arms rotated 22.5° relative to each other. The "foot" of the diagram, in the central foreground, represents strong signals in both interferometers. This is the region that corresponds to signals traveling close to vertically, and with stretch and shrink axes almost aligned with the arms of both interferometers.

The left histogram of Figure 4 is similar, except the coincident interferometers are rotated by a relative angle of 45°. Note that part of the foot has disappeared, because fewer sources can send waves that are close to optimally aligned, with interferometers misaligned by this (maximal) amount.

The right-hand histogram of Figure 4 is for two candidate sites, Edwards Air Force Base and Columbia, Maine. The relative alignment of the interferometer arms is selected to be optimal, as given by the "Coincident Projection Alignment" requirement that: *The detector arms make equal angles with the line of intersection of their planes, modulo 90°.* This prescription is equivalent to the following formulation of optimal alignment, given site latitude and longitude coordinates:

> Denote by (β_1, γ_1) and (β_2, γ_2) the (latitude, longitude) coordinates of two sites. Define $\overline{\beta} = (\beta_1+\beta_2)/2$, $\beta_- = (\beta_2-\beta_1)/2$, $\gamma_- = (\gamma_2-\gamma_1)/2$. Let $\mu_- = \mu_2-\mu_1$ be the difference in orientation, with positive μ_- indicating that interferometer

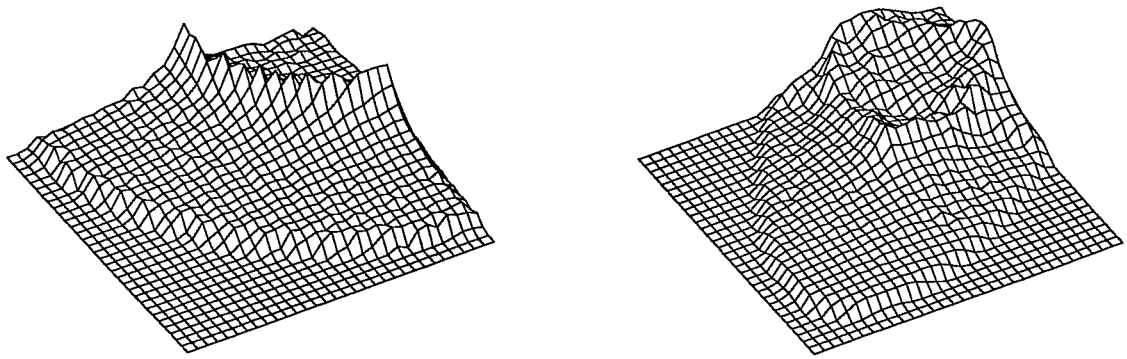

Figure 4: *Left:* Spatially coincident interferometers with relative rotation of 45°. *Right:* Edwards Air Force Base (A_1) and Columbia, Maine (A_2), with optimal relative orientation (Edwards rotated 33° to the west).

2's arms should be rotated counterclockwise on a conventional map relative to interferometer 1's by μ_-.

$$\mu_- = 2 \arctan \frac{\tan \gamma_- \sin \overline{\beta}}{\cos \beta_-} \tag{2}$$

For example,

$$(\beta_1, \gamma_1) = (34.95°, -117.78°) \quad \text{(Edwards)}$$
$$(\beta_2, \gamma_2) = (44.67°, -67.9°) \quad \text{(Columbia)}$$
$$\mu_- = 33.27° \pmod{90°}$$

So if Columbia's L-geometry bisector is oriented 20° East of North, then Edwards' should be 13.27° West of North, modulo 90°.

The right half of Figure 4, separated detectors optimally aligned, is similar to Figure 3, spatially coincident detectors that are misaligned. This is because, even with optimal alignment, interferometers at opposite ends of the continent are necessarily in different planes.

2. Definition of Coincidence Sensitivity

Raw data similar to that of the two-dimensional histograms above are reduced to a single sensitivity number. Qualitatively, the most sensitive configurations have a high event rate for the strongest signals in both interferometers (large foot). In searching for gravitational waves, the sources coming from the optimal direction (vertical) and with the optimal polarization (aligned with the arms) will be the most likely to be detected. Less optimal sources (such as those close to the nodes in one or both interferometers) will probably fall below the threshold for coincident detection. A sensitivity figure of merit for interferometer pairs should reflect

this property, giving weight to the region of the sky and the source polarization that gives strong signals in two interferometers, but not excluding such a large fraction of the sky that the probability of detection is significantly reduced.

Quantitatively, define the coincidence sensitivity as the detected signal level $A_0(x)$ in both interferometers which covers that portion of the sky (and polarization space) containing the fraction x of the strongest *detected* signals (all sources have inherent strength of unity)—see Figure 3.

3. Sensitivity as a Function of Separation

Figure 5 shows how the pair-sensitivity A_0 changes as the separation increases. Because of the symmetry of isotropic sources, the result depends only on the separation, not on the absolute latitudes or longitudes[3].

As the sky coverage x is increased from 0 to 0.50, the dependence on separation decreases. This is because increased sky coverage comes at the expense of including the part of the response patterns of the interferometers near the null lobes, and the added degradation resulting from the interferometers being in different planes is relatively small.

4. Optimal Threshold

In the discovery phase, the threshold settings for coincidence detection should be adjusted to maximize the chance of detecting sources. To give a rough idea of the optimization procedure, we make the following approximation:

The probability of detection P in a fixed time interval is $P \propto x{A_0}^m$.

In the approximation of a homogeneous distribution of sources, $m = 3$, but because of the concentration of sources in the Virgo cluster, $m \lesssim 2$ may be a more accurate estimate. As an example, consider optimally oriented interferometers with $\psi = 39°$ (the separation between Edwards and Maine); Figure 6, equi-sensitivity contours derived from the same data presented in Figure 5, yields the following table (the last two columns are normalized to the largest entries):

[3]When considering two sites and isotropic sources, the globe can be rotated to place both sites along the equator without affecting the results.

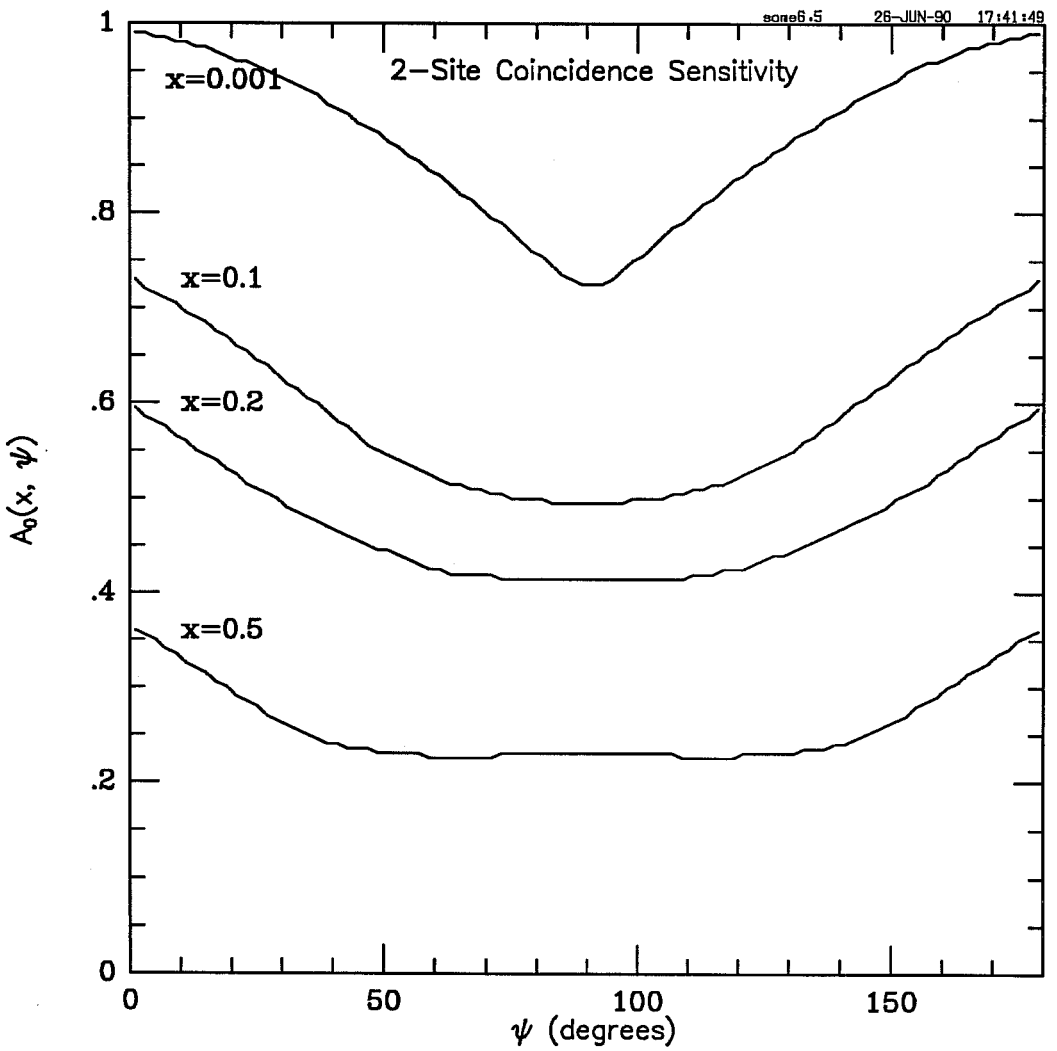

Figure 5: Sensitivity A_0 for an interferometer pair, as a function as the separation on the globe ψ and sky coverage x. Both interferometers have one arm parallel to the line of intersection of the interferometer planes, consistent with the "Coincident Projection Alignment" of Equation 2.

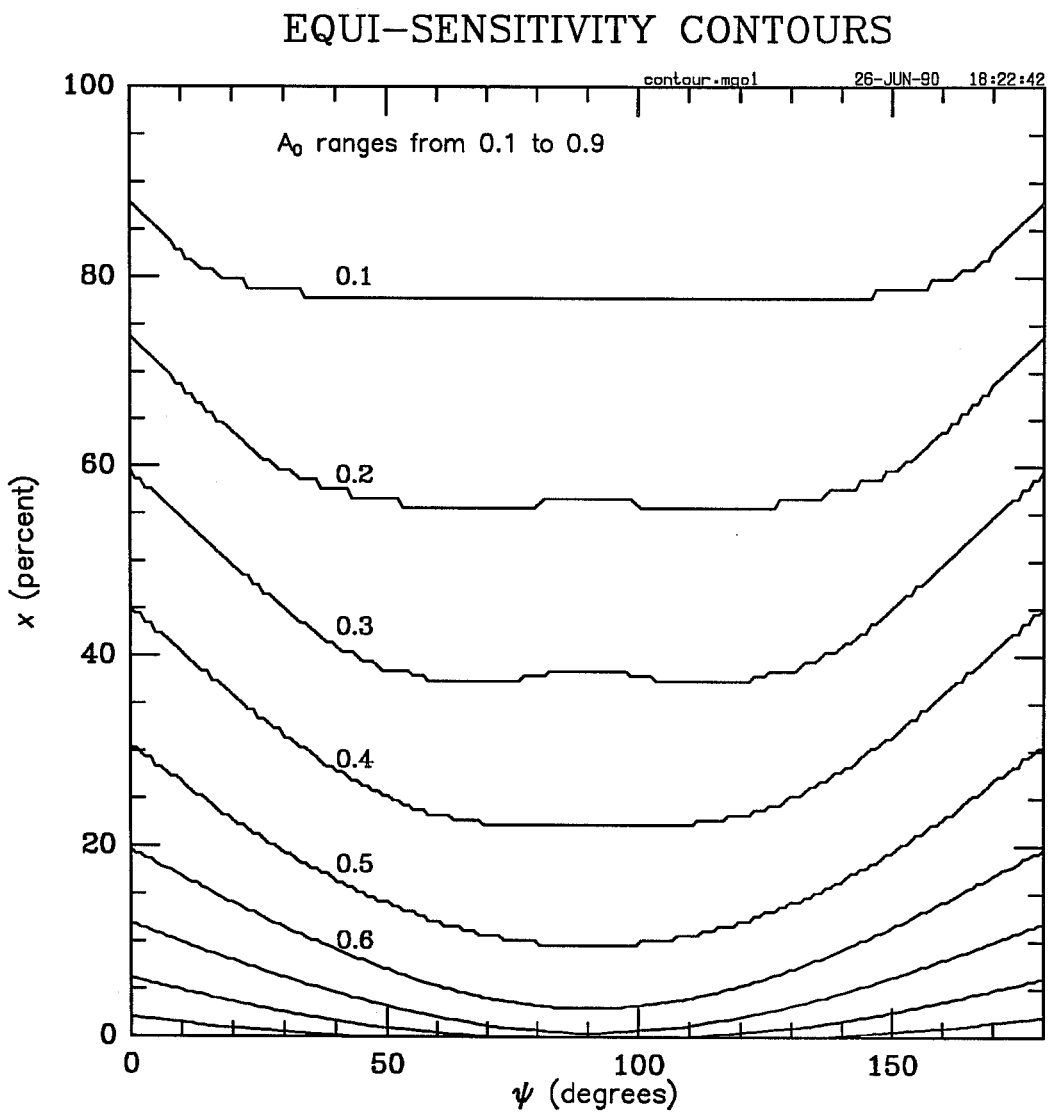

Figure 6: Constant-sensitivity lines for a pair of interferometers operating in coincidence. The orientations and variables are the same as in Figure 5.

A_0	x	$xA_0{}^2$	$xA_0{}^3$
.1	.78	.17	.04
.2	.58	.51	.22
.3	.42	.84	.5
.4	.28	1	.9
.5	.17	.9	1
.6	.09	.7	.9
.7	.05	.6	.8
.8	.02	.3	.5
.9	.001	.02	.05

The table indicates that, depending on the distribution of sources and other factors, the threshold should be in the range $0.3 \lesssim A_0 \lesssim 0.6$, corresponding to the sky coverage range $.4 \gtrsim x \gtrsim .1$. For comparison purposes in the next section, we take $x = 0.2$.

5. Sensitivity as a Function of Orientation

Figure 7 shows how the coincidence-sensitivity A_0 changes with orientation of the interferometer arms. Four site pairs are shown. Each of the curves is the sensitivity for a sky coverage $x = 0.20$. They are normalized to the one-site curve (by dividing by the optimum value $A_0 = 0.60$ for $x = 0.20$).

For detectors separated by $\psi \lesssim 40°$, the coincidence sensitivity A_0 changes by less than 3%, as long as the *relative* orientation for coincidence alignment specified by Equation 2 is maintained. Figure 8 illustrates the effect of *absolute* alignment for larger separations, by comparing the sensitivity given two orientations of Site 1 (in this case Hanover) that differ by 45°.

Site 1	Site 2	ψ	$A_{0,\,\max}(\mu_1 = 0°)$	$A_{0,\,\max}(\mu_1 = 45°)$	$\Delta(A_0)$
Hanover	Maine	49°	.74	.74	$\lesssim 1\%$
Hanover	Edwards	81°	.70	.65	7%

Also apparent from Figure 8 is the following conclusion

> The maximum variation in sensitivity as a function of orientation for site pairs separated by $50° \lesssim \psi \lesssim 80°$ is approximately 15% (the difference between maximum and minimum alignment).

Figure 7 demonstrates that as the separation between the sites increases, the sensitivity becomes less dependent on relative alignment. This is because there is no good optimum alignment for detectors in different planes. For a similar reason, the sensitivity maximum is a sharper function of orientation than is the minimum sensitivity. In misaligned detectors, sources from a larger fraction of the sky contribute equally.

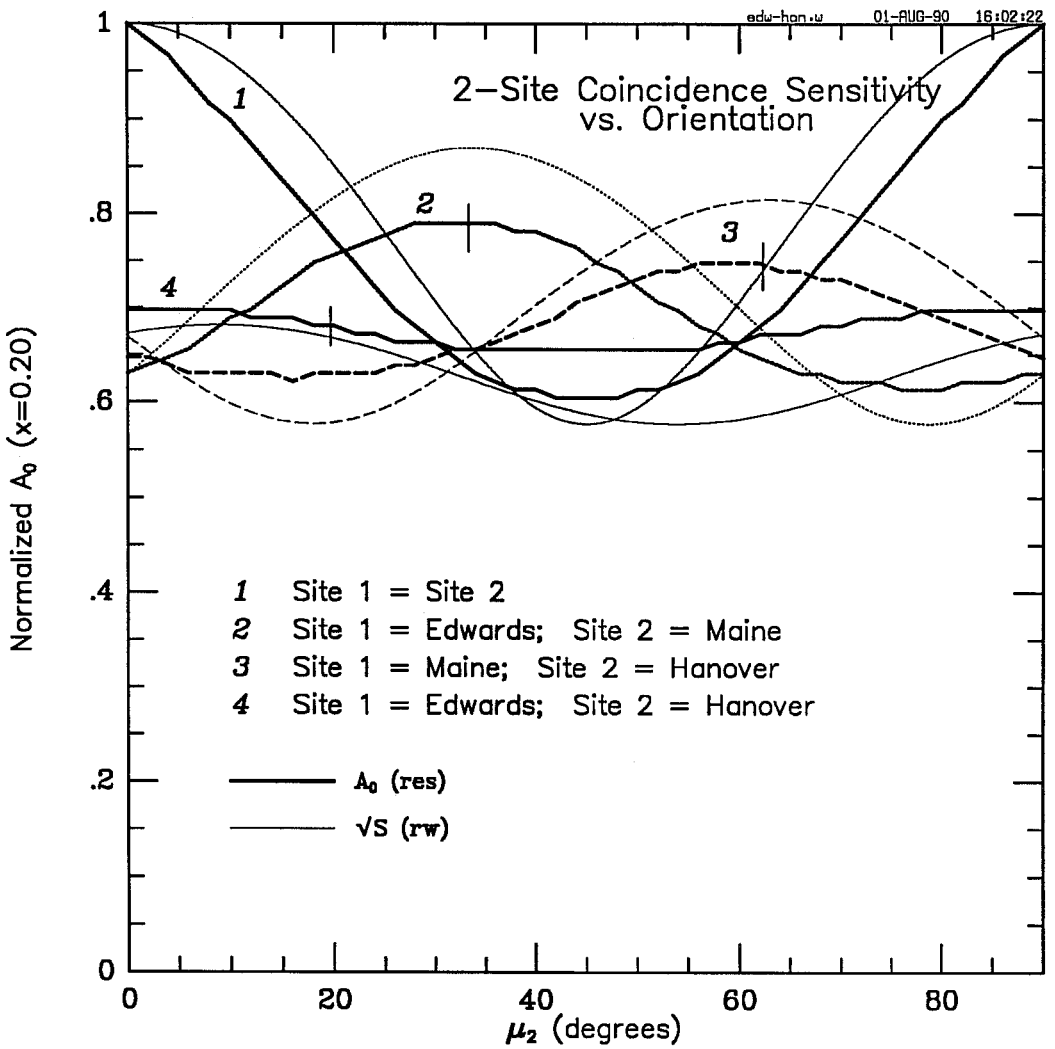

Figure 7: Sensitivity of an interferometer pair as a function of compass direction of the arms. The Site 1 interferometer has its bisector pointing to local North ($\mu_1 = 0°$), and the Site 2 bisector varies from North to East. The shapes of the curves are only slightly sensitive to the value of μ_1—see Figure 8. The sky coverage is fixed at $x = 20\%$. All curves are normalized relative to $A_0 = 1$ for the Site 1 = Site 2, aligned case. The vertical bars mark the coincidence projection alignment for maximum sensitivity, as given by Equation 2. The heavy lines are the result of the calculations described in this report; the light lines are the calculation of Weiss and Christensen.

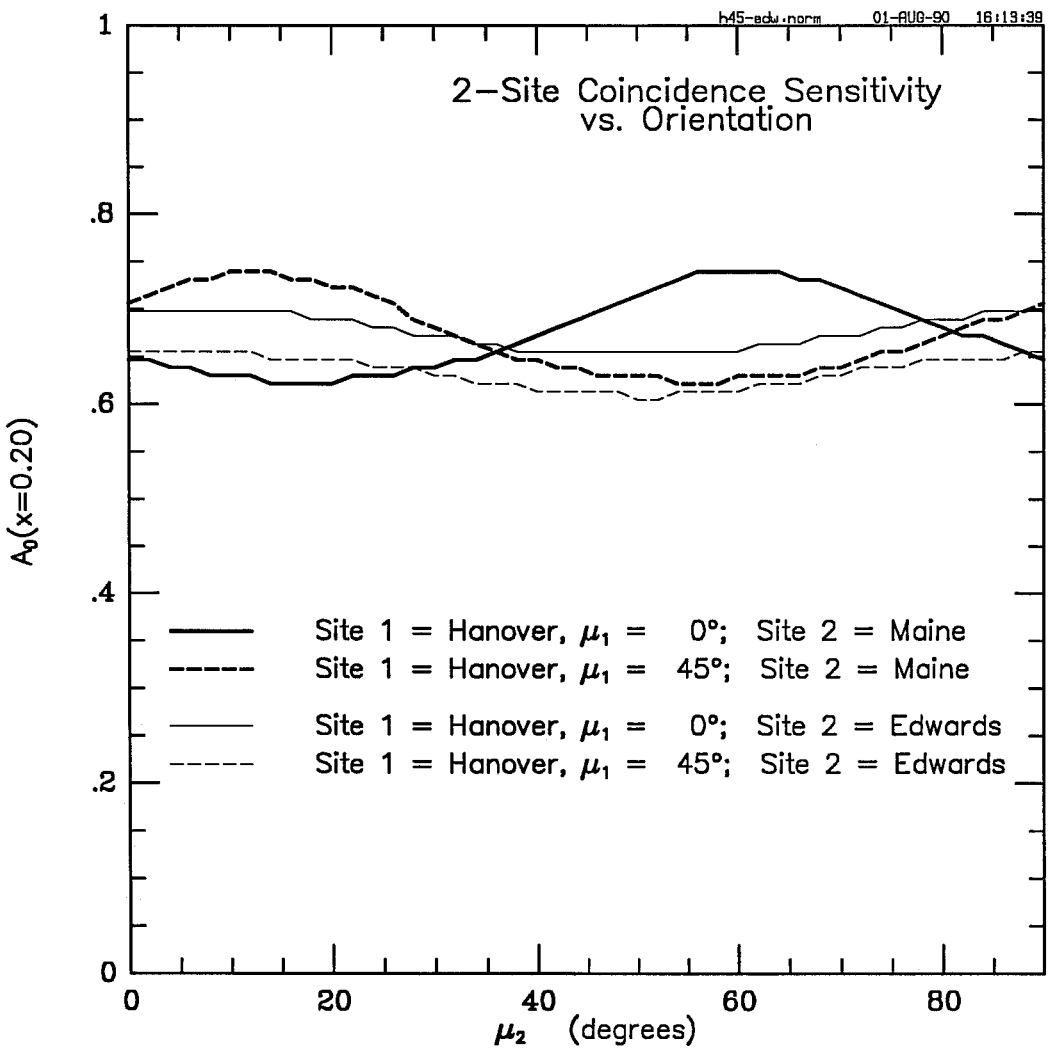

Figure 8: Demonstration of the increasing importance of absolute orientation as the separation of sites ψ increases. The pair of heavy curves represents the sensitivity of Hanover and Maine interferometers operating in coincidence, with two different orientations for Hanover. To first order, the dashed curve is the same as the solid curve, but shifted along the μ_2 axis by $\Delta(\mu_1) = 45°$. The lighter curves represents the same sensitivity calculation, but for Hanover and Edwards—a pair with greater separation ψ.

6. Comparison with Other Formulations

Related analyses have been done by Schutz and Tinto [1], Christensen and Weiss [2], and Y. Gürsel and M. Tinto[3].

6.1. Nomenclature

Quantity	This Report	Weiss/Christensen	Gürsel/Tinto
Bisector Angle	μ	"bisector azimuth"	$\alpha - 90°$
Angular Separation on Globe	ψ	b	
Sensitivity	A_0	S_2	"relative threshold" $T_{\rm rel}$
Sky Coverage	x		$C(T_{\rm rel})$

6.2. Definitions of Sensitivity

The original work of Schutz and Tinto [1] defined an average coincidence probability, which gives details of the response of various detector pairs to orintation but is not directly translateable into detector sensitivity.

The work of Gürsel and Tinto [3] addresses the issue of a properly weighted average coincidence probability by averaging over an isotropic homogeneous distribution of sources. They define the "Detection Efficiency" N as

$$N = \int_0^1 C\left(\frac{r}{R}\right)\left(3\left[\frac{r}{R}\right]^2\right) d\left[\frac{r}{R}\right] \tag{3}$$

Following a suggestion of Kip Thorne[4], this result can be converted to sensitivity A_0 by $A_0 = N^{1/3}$. Making this conversion, there is good (within 5%) agreement between their results and the results presented of this report.

Weiss and Christensen [2] define sensitivity as "the product of strains squared averaged over an isotropic source distribution", Christensen's "Method B:"

$$\sqrt{S_2} = \left(\int_0^{2\pi} d\phi \int_0^{\pi} \sin\theta\, d\theta \left[F_{1+}^2 F_{2+}^2 + F_{1\times}^2 F_{2\times}^2\right]\right)^{1/2} \tag{4}$$

The result of this simple analytic formulation is shown for comparison as the light set of lines in Figure 7.

7. Conclusions and Other Considerations

If optimal alignment can be obtained, increasing the separation between detectors reduces the coincidence sensitivity of a pair of interferometers by 20% to 30%, for continental or larger separations, relative to spatially coincident interferometers. This is the effect for

[4]Private communication, 1 July, 1990.

linearly polarized sources; for elliptical polarization, the reduction in sensitivity is smaller, perhaps becoming insignificant for a large class of sources.

Another advantage of placing the sites close together is improved timing resolution, and a consequent reduction in the accidental rate from noncorrelated interference. Also, the optimal separation for searching for a stochastic background may be on the order of 100 km. On the other hand, the advantages of increasing the separation are better spatial resolution when operated in a network of three or four interferometers and better rejection of correlated backgrounds.

References

[1] Bernard F. Schutz and Massimo Tinto, "Antenna patterns of interferometric detectors of gravitational waves—I. Linearly polarized waves" *Mon. Not. R. astr. Soc.* (1987) **224,** 131–154.

[2] R. Weiss, untitled memo dated 17 June, 1990

[3] Y. Gürsel and M. Tinto, Draft report *Detection efficinecy of a pair of laser interferometric gravitational wave detectors operating in coincidence as a function of their orientations*, 21 June 1990.